Laser Papers from AIAA 9th Aerospace Sciences Meeting

The following seven articles are from the two Laser Sessions of the AIAA 9th Aerospace Sciences Meeting that was held in New York, N.Y., January 25–27, 1971. The Editor and staff of AIAA Journal wish to thank Jerzy S. Gruszcynski of the General Electric Company for his outstanding efforts as Guest Editor for this group of papers.

Experimental Gas Dynamic Laser Studies

RICHARD A. MEINZER*
United Aircraft Research Laboratories, East Hartford, Conn.

In this paper the results of some experimental measurements on the CO_2–N_2–H_2O gas dynamic laser (GDL) are reported. These measurements were performed using a small-scale "mini-rocket" located in a laboratory test facility which is also described. In the combustion chamber of the rocket engine, CO and H_2 are burned with O_2 to form CO_2 and H_2O; N_2 is added as a diluent so that the temperature of the resulting mixture is of the order of 1500°K. The supersonic expansion of the thermally hot gas mixture of CO_2, N_2, and H_2O results in a population inversion in the CO_2 gas molecules. This population inversion has been characterized by gain measurements. The results of the experimental gain measurements are presented as plots of gain vs gas composition, stagnation pressure, and frequency. Some comparisons of the experimental gain measurements are made with theoretical calculations. In addition, the results of some oscillator experiments are described wherein the optical power is measured as a function of mass flow, gas composition, frequency and area ratio. Also, the effect of using fuels and oxidizers other than CO and O_2 is discussed.

Nomenclature

a = gain coefficient at line center, %/cm
a_0 = small-signal gain coefficient at line center, %/cm
B_1 = rotational constant for the 001 vibrational level
B_2 = rotational constant for the 100 vibrational level
c = speed of light
h = Planck's constant
I = probe laser intensity after passing through exhaust, w/cm^2
I_0 = probe laser intensity, w/cm^2
I_s = saturation parameter, w/cm^2
J = rotational quantum number
L = length of optical active region, cm
N_1 = number of molecules/cc in 001 level
N_2 = number of molecules/cc in 100 level
T_{rot} = rotational temperature, °K

Introduction

RECENTLY the concept of freezing molecular vibrational energy via a supersonic expansion has been utilized in the development of a gas dynamic CO_2 laser.[1–5] This laser is of interest because it utilizes thermal energy released from a chemical reaction for molecular excitation. The thermal energy is generated in the combustion chamber of a rocket engine, such as that shown in Fig. 1 in which CO and H_2 are burned with O_2 to form CO_2 and H_2O; N_2 is added as a diluent so that the temperature of the resulting mixture is of the order of 1500°K. At the subsonic gas velocities attained in the combustor, thermodynamic-equilibrium is established so that a substantial fraction (of the order of 10%) of the N_2 molecules are vibrationally excited as a result of the high combustor temperature. The gas mixture then undergoes rapid aerodynamic expansion through the supersonic nozzle of the rocket engine and the vibrational energy which the nitrogen molecules attained in the combustor is effectively frozen near combustion chamber conditions. This reservoir of vibrational energy stored in the nitrogen molecules is available to pump the 001 level in CO_2 during molecular collisions through the mechanism of near-resonant vibrational energy transfer. The lower lasing level (100), on the other hand, is maintained near equilibrium in the rapidly expanding and cooling flow as a consequence of the presence of a small concentration of H_2O which is known to be effective in relaxing the 0V0 level[6] and, hence, also the 100 level of the CO_2 molecules. The simultaneous pumping of the 001 level and deactivation of the 100 level establishes a population inversion in the flowing medium. This particular flowing medium is especially useful in that very high powers can be extracted from a relatively small volume of gas. The results of an experimental investigation of this flowing medium which is generated by the exhaust of a rocket engine are presented in this paper.

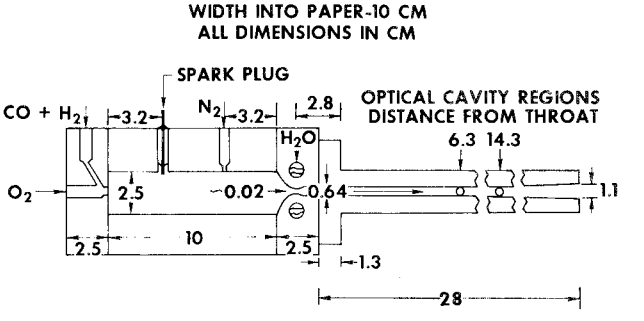

Fig. 1 Minirocket GDL showing original combustor.

Presented as Paper 71-25 at the AIAA 9th Aerospace Sciences Meeting, New York, January 25–27, 1971; submitted January 25, 1971; revision received December 20, 1971. This work was sponsored in part by UARL and in part by the Air Force Weapons Laboratory, Air Force Systems Command, Kirtland AFB, N.M., and the Advanced Research Projects Agency. The author wishes to thank J. D. Anderson, Jr., Chief of the Hypersonics Group in the Aerophysics Division at the Naval Ordnance Laboratory, White Oak, Silver Spring, Md. both for making available his computer program and for performing the theoretical calculations presented herein.

Index categories: Lasers; Thermochemistry and Chemical Kinetics; Nozzle and Channel Flow.

* Research Scientist, Chemical Sciences Section.

Apparatus

Test Facility

All gas dynamic laser (GDL) tests were conducted in the vacuum-tight test facility shown schematically in Fig. 2. Use of this test facility protected laboratory personnel from exposure to carbon monoxide in the event of leaks in the rocket engine, and the large ballast tank greatly increased the static pressure range over which small scale minirocket tests could be conducted by increasing the available run time at a given pressure level. This test facility could be easily evacuated to less than 0.2 torr and would maintain blank-off pressures of this magnitude. In actual tests, the static pressure was varied from approximately 4 torr to more than 50 torr at flow rates from 0.005 lb/sec to 0.2 lb/sec.

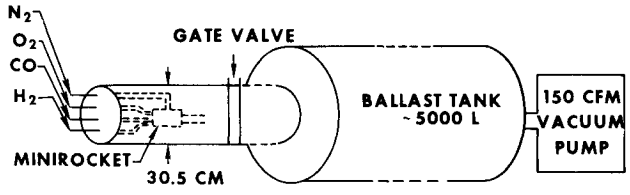

Fig. 2 Minirocket test facility.

Rocket Engine and Nozzle

A schematic diagram of the minirocket GDL is shown in Fig. 1. Internally, the combustion chamber, made of copper, is 10 cm long, 2.5 cm high and 10 cm wide. Carbon monoxide, hydrogen, and oxygen are mixed in the rear of the combustor. They are ignited by a spark plug which is located approximately 3.2 cm from the injector. Nitrogen is introduced 3.8 cm beyond the spark plug and enters the combustor through two multi-holed injectors, which are not shown. The nozzle and associated duct are bolted to the combustor. This combustor worked well with the two-dimensional nozzle (shown in the figure) to a stagnation pressure of approximately 12 atm. At pressures above 12 atm results were obtained which indicated that poor mixing might be occurring within the combustor. Similar results were obtained with other nozzle configurations. For this reason, a second combustor was constructed and is shown in Fig. 3. This second combustor

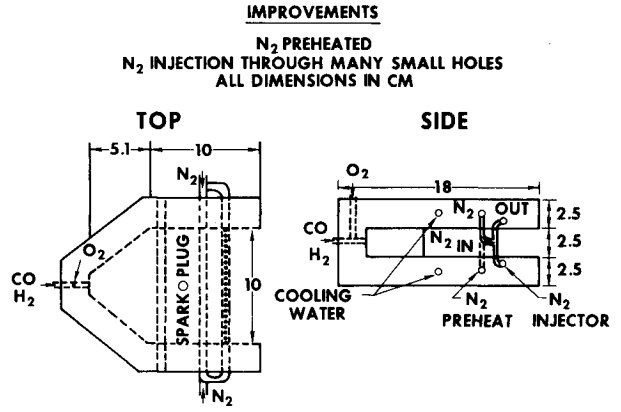

Fig. 3 Improved combustor.

appeared to eliminate the spurious data trends observed with the first combustor at high pressures, as had been anticipated. The representative data chosen for inclusion in this paper do not substantiate this contention as well as some that were omitted. Below 12 atm results obtained with the two combustors were identical. Probably, improved mixing was achieved in this second combustor by introducing the N_2 through a series of small holes in the rocket engine housing, as indicated in Fig. 3. This new combustor had the additional advantage that the nitrogen gas was preheated by passage through the engine block before it entered the combustion chamber through the injection holes. The effect of preheating the nitrogen in this manner was to recover some of the heat lost to the rocket engine housing, and thereby achieve higher combustion gas temperatures. Some miscellaneous experiments were performed with both the original and improved combustors, in which both the length of the combustor and the nitrogen injection ports were varied. No significant increases in the magnitude of the gain coefficient over that measured with the improved combustor were observed. Unless otherwise stated, this improved combustor was used to obtain all data presented in this paper that were measured at high stagnation pressures.

Propellant Supply

All gas flows, with the exception of that for hydrogen, were measured by choked orifices, which were periodically recalibrated. At very low flow rates, hydrogen was introduced into the combustion chamber via a flowmeter. Each gas flow rate can normally be monitored with an accuracy of better than 5%. In certain cases, the magnitude of this uncertainty can be reduced to 1%. Unless otherwise stated, all tests were performed by burning carbon monoxide and hydrogen with 10% more oxygen than needed for stoichiometry. Nitrogen was added to the combustion products. In all cases the gases used were those supplied by the manufacturer without additional purification. The manufacturer's quoted purity on each gas was as follows: CO, 99.5%; N_2, 99.7%; O_2, 99.6%; and H_2, 99.9%.

Measurements

Gas Dynamic Measurements

Stagnation temperature measurements were made by a thermocouple, which was inserted into the combustion chamber. The temperatures thus obtained have agreed with values obtained via a stagnation temperature probe placed in the supersonic flow. The Mach numbers have been determined in a few cases from the ratio of stagnation pressure to the Pitot pressure. Resulting values agreed well with theoretical predictions based on the area ratio corrected for boundary-layer growth. Static pressures are measured at the side of the duct where the probe laser beam enters or else at the center of the duct above the path of the probe laser beam. Estimates of the Mach number, based upon the ratio of stagnation pressure to static pressure, have agreed in general with the results of other types of measurements. Throat areas have been measured with feeler gauges when the engine was not running and calculated from the stagnation pressure P stagnation temperature T composition, and flow rate W using the equation

$$A = W(T)^{1/2}/Pf(\gamma) \tag{1}$$

where $f(\gamma)$ is a function of the heat capacity ratio. In general, good agreement has been obtained between these two methods of determining throat area.

Shadowgraphic Measurements

In some cases, shadowgraphs have been obtained of the rocket-exhaust along the path of the probe laser. These measurements were made in the usual manner and then compared with theoretical predictions.[7]

Gain Measurements

All gain measurements were made by using a single-frequency probe laser. The probe laser is an ordinary CO_2 electric discharge laser which is specially designed to provide amplitude stability.[8] It was operated on a single frequency (a single P transition) which was measured with a Perkin-Elmer Model 98 spectrometer. The frequency can be varied in increments over a range of frequencies

corresponding to approximately six different P transitions. At all times the probe laser beam was oriented perpendicular to the gas flow. Whenever it is not so oriented, a reduction in gain is observed, which is theoretically predicted by taking the Doppler shift into account. The size of the probe beam was determined by an iris, which was located just before the probe beam enters the rocket exhaust. The reproducibility of gain measured in this way is, in general, approximately $\pm 0.04\%\ \mathrm{cm}^{-1}$.

The gain was calculated from the experimentally measured ratio of the intensity of the probe laser beam when it passed through the rocket exhaust with the engine running I to that when the engine was not running I_0 using the equation

$$I/I_0 = e^{aL} \tag{2}$$

where L is the length of the rocket exhaust which is traversed. The gain a is given by the following equation[9]

$$a = a_0/(1 + I/I_s) \tag{3}$$

where a_0 is the small signal gain and I_s is a saturation parameter. For the experiments described in this paper, I_0 was equal to approximately $\frac{1}{2}\ \mathrm{w/cm^2}$ and I_s was measured to be of the order of $1000\ \mathrm{w/cm^2}$. Since I was never more than 10% larger than I_0, a was essentially equal to a_0, and all the quoted gains are the small-signal values. The frequency of this probe laser was adjusted to give the peak gain at each P transition.

Results and Discussion

Gain vs Composition

A large number of measurements were made to determine the value of the small signal gain as a function of gas composition in the laser cavity. Representative results are presented in Fig. 4, which shows experimental gain measurements for various CO_2/H_2O ratios at 70 mole percent nitrogen. The data in Fig. 4

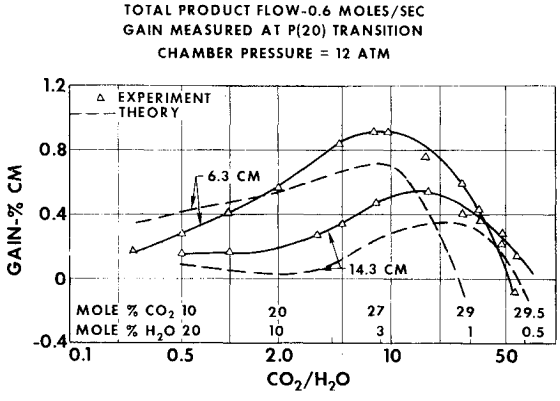

Fig. 4 Gain vs CO_2/H_2O ratio at 70 mole $\%N_2$.

give results obtained at both 6.3 cm and 14.3 cm from the throat. The measurements were made at a frequency corresponding to the P (20) transition. They were made with a constant product mass flow rate of 0.6 mole/sec, which corresponds to a stagnation pressure between 12.3 and 12.8 atm, depending on composition and temperature. A comparison of the two curves presented in the figure shows that at low percentages of H_2O (high CO_2/H_2O ratio) the gain decays more slowly with distance than at high water concentrations (low CO_2/H_2O ratio). The reason for this behavior is that the water at low concentrations essentially only deactivates the lower lasing level, whereas at high water concentrations the upper level is also depopulated, which causes the gain to decrease at large water concentrations. At very low H_2O concentrations not enough water is present to fully deactivate the lower laser level; consequently, the gain goes to zero. The reason gain is observed at lower water concentrations at 14.3 cm, compared to 6.3 cm from the throat, is that more time is available in the former case for deactivation of the lower laser level to occur.

The dotted lines in Fig. 4 give the results of a theoretical calculation of the gain for the conditions at which the experiment was conducted. The theoretical gain curves were calculated by inputting the gas composition, stagnation temperature, stagnation pressure and nozzle contour into a computer program developed by Anderson.[10–12] The rate constant data tabulated by Taylor and Bitterman[13] were used for all relaxation rates except for the vibrational relaxation of CO_2 by H_2O. For this process the rate calculated by Sharma[14] was used. The theoretical gain numbers presented in the figure were reduced by approximately 10% to correct for the effect of Doppler broadening which becomes important at low static pressures. A comparison of the theoretical and experimental cases in Fig. 4 shows some qualitative agreement. Both the experimental and theoretical gains are higher nearer the throat than they are downstream of the throat. At very low water concentrations both the theoretical and experimental gain decrease as the water concentration is further reduced. The fact that the experimental and theoretical gains are almost identical at low water concentrations at 14.3 cm from the nozzle throat implies that the water deactivation rate might be in error. A comparison of the peak gain, which is not presented in this paper, with the experimental gain implies that a factor of 2 change in the water deactivation rate might greatly enhance the quantitative agreement between the theory and experiment. This explanation is further developed in the discussion of Fig. 8.

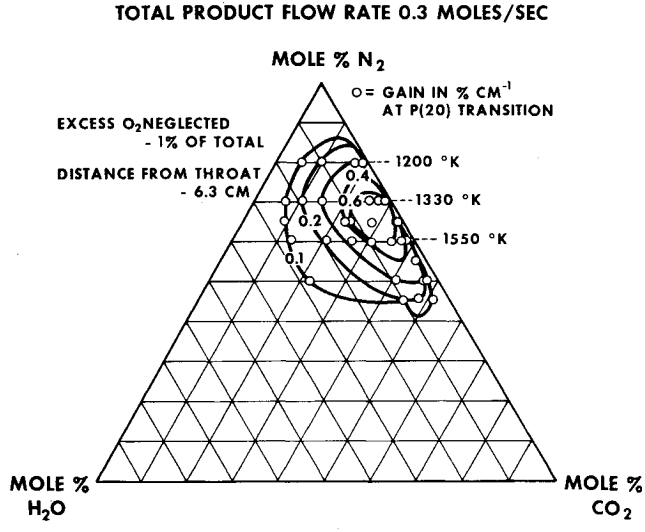

Fig. 5 Experimental gain variation with combustion product composition.

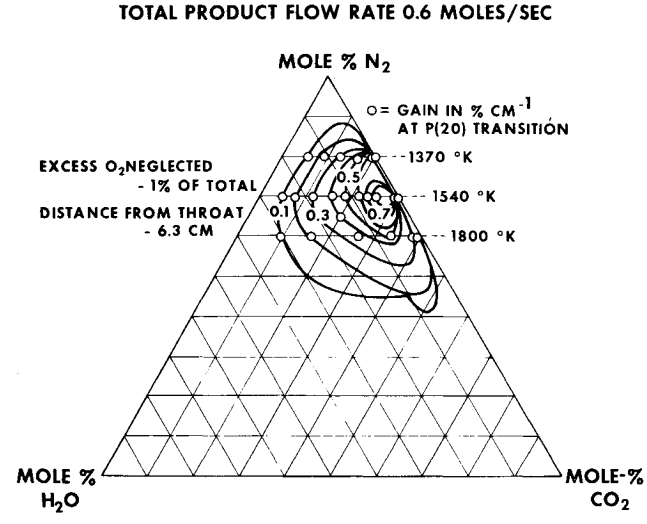

Fig. 6. Experimental gain variation with combustion product composition.

The data presented in Figs. 5 and 6 summarize much of the experimental gain data which have been collected to date on the copper nozzle shown in Fig. 1. The three corners of the equilateral triangle correspond, respectively, to 100% of the constituent listed there. The side opposite to the apex corresponds to 0% of the respective constituent. The data presented in these figures was originally obtained in the form presented in Fig. 4, i.e., the gain was measured as a function of CO_2/H_2O ratio at different percentages of nitrogen. In Fig. 5 the data obtained at total product mass flow of 0.3 mole/sec (stagnation pressure of 2.7 to 7.7 atm) is presented and in Fig. 6 the data obtained at 0.6 mole/sec (stagnation pressure of 8.9 to 15.3 atm) is presented. The measured stagnation temperatures associated with different percentages of nitrogen are given to the right of each plot. As the CO_2/H_2O ratio was varied at a constant percentage of nitrogen, the stagnation temperature remained almost constant, since the molar heats of combustion of CO and H_2 are nearly the same. Some of the parts of the contour lines in Fig. 6 were extrapolated from data presented in the preceding figure.

Gain vs Frequency

A typical variation of measured gain with wave length is given in Fig. 7. The theoretical variation of gain with frequency is a function of rotational temperature, as given by the following equation[15]

$$a=\frac{(\text{const})}{T_{\text{rot}}}J\left[N_1B_1\exp\frac{-B_1hcJ(J-1)}{kT_{\text{rot}}}-N_2B_2\exp\frac{-B_2hcJ(J+1)}{kT_{\text{rot}}}\right]$$

From the shape of the curve, the rotational temperature was estimated to be 331 ± 20°K. From independent gas dynamic measurements (pitot pressures, static pressures, and stagnation temperatures), the static temperature was estimated to be 320 ± 10°K. Therefore, the data in Fig. 7 indicate that, within

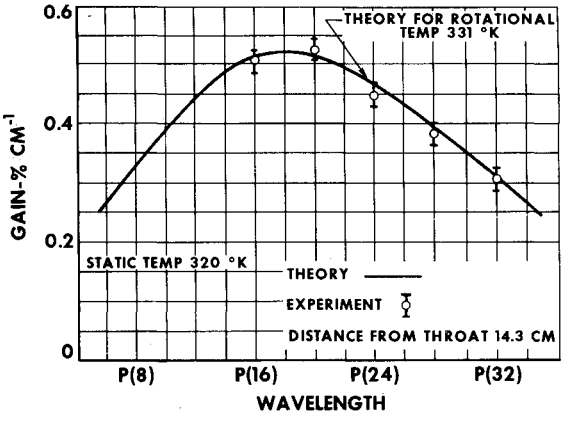

Fig. 7 Representative curve of gain vs wavelength.

the experimental error, these two temperatures are equal. This equality implies, as expected, that a Boltzmann distribution exists among the rotational levels of the carbon dioxide molecules at a temperature approximately equal to the static temperature. This type of measurement has been made at several distances from the throat and at different stagnation pressures. To date, all measurements have given the same type of results as shown in Fig. 7.

Gain vs Stagnation Pressure

In Fig. 8 are presented representative data on the variation of gain with stagnation pressure. The data were obtained using the combustor described in Fig. 1. The sudden reduction in gain at a stagnation pressure of approximately 12 atm is believed to have been a consequence of poor mixing within the combustor. When the modified combustor illustrated in Fig. 3 was used, the dip in the curve at 12 atm and above was not observed, and the gain

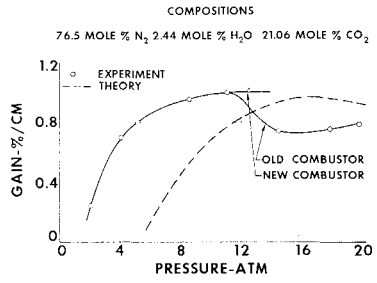

Fig. 8 Gain $P(20)$ transition vs stagnation pressure at 6.3 cm from nozzle throat.

essentially followed the heavy line. However, at pressures of less than 12 atm the results obtained with the two combustors were identical. With the test conditions of Fig. 8, the highest gain reported to date in a GDL, namely, $1.0 \pm 0.04\%\,\text{cm}^{-1}$, was attained.

The theoretical gain curve presented in Fig. 8 was calculated as described in the discussion of Fig. 4. A comparison of the theoretical and experimental gain presented in Fig. 8 indicates good agreement at high stagnation pressures and poor agreement at low stagnation pressures. A comparison of the theoretical peak gain, which occurs further downstream of the nozzle exit plane the lower the stagnation pressure, with the experimental results shows almost quantitative agreement. The distance from the nozzle exit plane to the point where the peak gain occurs can be reduced by increasing the rate of vibrational relaxation of the 100 level of CO_2 by H_2O. As discussed previously a factor of 2 change in the water deactivation rate is estimated to be sufficient to move the location of the theoretical peak gain so that the quantitative agreement between theory and experiment will be greatly enhanced.

Gain vs Fuel/Oxidizer Ratio

In Fig. 9 are shown representative data on the variation of gain and stagnation temperature with the CO mole flow rate. In those tests the flow rate of N_2, H_2, and O_2 injected remained constant.

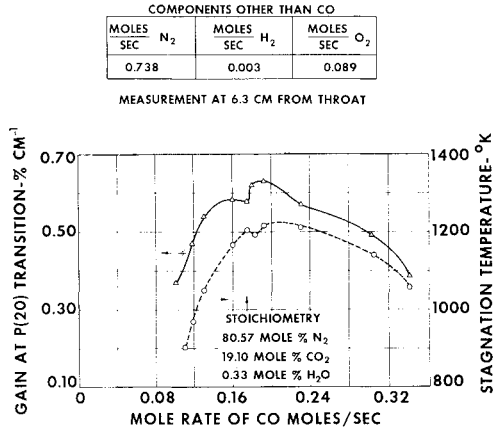

Fig. 9 Representative plot of experimental gain and stagnation temperature vs number of moles of CO as fuel in inlet mixture.

The gain peaks reproducibly on the fuel-rich side of stoichiometric conditions. The gain then decreases as more excess CO is added. Apparently, the decrease in gain parallels the reduction in stagnation temperature within the combustor. The peaking of the gain on the fuel-rich side of stoichiometric conditions suggests that the CO is pumping the CO_2 just as the N_2 does. Thus, the gain increases with a small excess of CO, just as it would with an increment of N_2.

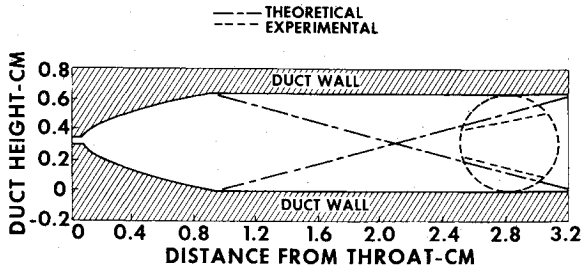

Fig. 10 Theoretical and experimental location of shock waves in nozzle.

Shadowgraph

The results of a typical shadowgraph measurement made on the two-dimensional copper nozzle are shown in Fig. 10. The theoretical curve was obtained with a computer program which uses the method of characteristics to solve the gas dynamic equations needed to calculate the flowfield downstream of the nozzle throat. The theory is compared with the experiment at approximately 2.8 cm from the throat. The dashed circle represents the aperture available to the experiment. The magnitude of the gain measurements and power measurements to be described subsequently was significantly reduced when the laser beam passed through the region of crossing shock waves; consequently, this region was avoided in taking representative data.

Laser Power vs Mole Flow Rate

In addition to the large number of gain measurements which have been made on the gas dynamic laser, a number of laser output power measurements have also been made. These power measurements were made with a Coherent Radiation Laboratories Model 201 power meter, which has an accuracy of $\pm 5\%$ and has a flat response over the wavelength range from 0.3 to 30 μ. The power extracted by the optical cavity was transmitted into the power meter after passing through a salt window which separated the low pressure region inside the test facility from the atmosphere. The optical cavity consisted of two mirrors separated by approximately 18 in.; one mirror was a total reflector with the radius of curvature indicated in the figure and the other was a flat surfaced partial reflector whose transmittance is also indicated in the figure. One of the first power measurements to be made was a measurement of the power as a function of mass flow or chamber pressure. The results of a representative set of measurements are given in Fig. 11, which is a plot of power vs moles/sec of mass flow through the combustor. As expected, the power increases approximately linearly with flow rate for the three different gas compositions illustrated in Fig. 11. However, different power levels are attained with the different mixtures, because the system gain is a function of the gas composition, as had been indicated in the preceding figures giving the results of the gain measurements. The highest power generated by the laser

COMPOSITION	A	B	C
CO_2	22.1 MOLE %	20 MOLE %	16.95 MOLE %
H_2O	4.95	10	16.95
N_2	72.95	70	66.1

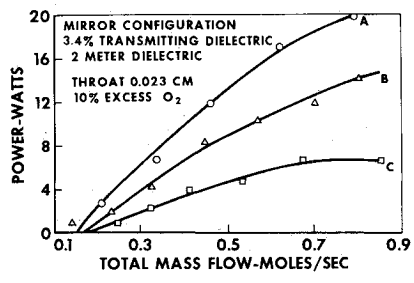

Fig. 11 Optical power output vs mole flow rate.

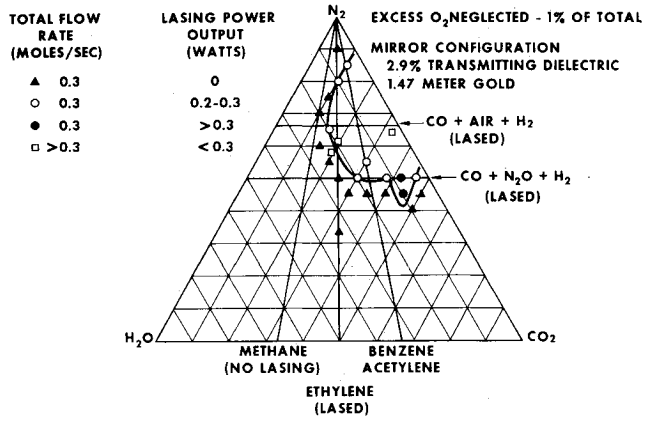

Fig. 12 Range of combustion for lasing.

is of the order of 50 w at a flow rate of 0.7 mole/sec with a gas composition differing only slightly from composition *A* listed in Fig. 11. However, the mirror transmisivity was reduced by approximately 1% from that indicated in Fig. 11.

Range of Composition for Lasing

In Fig. 12 is presented the range in composition over which lasing has been observed. A number of discrete mixtures of $CO + H_2 + O_2 + N_2$ were burned and the results of the lasing output power measurements were indicated by various symbols in the figure. The solid line represents an estimate of a contour of constant power. This contour line can be compared with results of gain measurements presented in Figs. 5 and 6. From the range of composition observed for lasing, it is obvious that fuels other than CO and H_2 can be used. As indicated in the figure, ethylene has been successfully used in place of CO and H_2. The solid line above ethylene represents the resulting product composition when ethylene is burned with O_2 and various percentages of nitrogen are added. Also, lasing has been achieved by burning the CO and H_2 with air instead of O_2. The solid line represents the burning of CO and H_2 with air. The O_2 can also be replaced with N_2O as indicated in the figure and lasing is still achieved. The only requirements to achieve a lasing medium are the presence of the combustion products, H_2O, CO_2, and N_2 at the appropriate mole ratio, temperature, and pressure.

In Fig. 13 is shown the actual laser power obtained by burning ethylene with oxygen and adding various percentages of nitrogen. The region over which lasing was obtained is in approximate agreement with the qualitative description given in the preceding figure. The data corresponding to a mass flow of 0.3 mole/sec should be used for the comparison. Data were obtained for two total mass flow rates of 0.3 mole/sec and 0.6 mole/sec. The higher powers were obtained at the larger flow rate because of the correspondingly greater chamber pressure. This result is in agreement with the data presented in Fig. 8 which gave the variation in gain as a function of stagnation pressure.

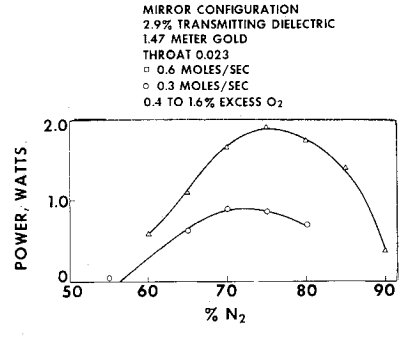

Fig. 13 Lasing power output vs $\%N_2$ for the combustion of ethylene with oxygen.

Also, it should be noted that at the larger mass flow rates, higher chamber temperatures were achieved because the percentage of heat losses to the rocket engine housing decreased with flow rate. In general, the power increases with chamber temperature to approximately 1500°K and thereafter decreases slightly.

Laser Power vs Area Ratio

Some estimate of the effect of area ratio on the performance of a GDL was obtained by varying the throat height of the nozzle, and some representative results are given in Fig. 14. The throat heights 0.018, 0.023, 0.025 cm correspond, respectively, to the area ratios of 36, 28, and 25. However, it should be pointed out that the nozzle was originally contoured for an area ratio of 30, and thus deviation from this value can cause some flow disturbance. The optimum area ratio appears to be of the order of 30, as indicated by the fact that the maximum power was achieved with a throat height of 0.023 cm.

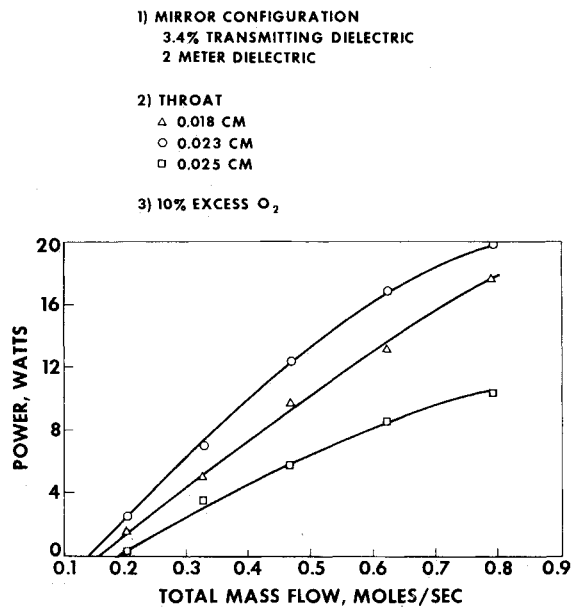

Fig. 14 Lasing power vs mass flow for different throat heights.

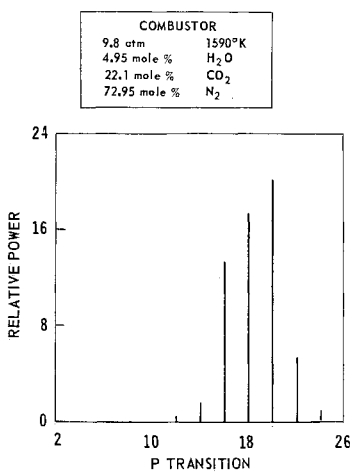

Fig. 15 Laser power vs wavelength.

Laser Power vs Frequency

The laser output power was scanned with a Perkin-Elmer 98 monochromater, modified for use with a grating blazed at 11 μ. The results of a typical run are presented in Fig. 15, which shows the laser power vs wavelength (P-transition). The maximum power was obtained at the -20 transition, which is the same transition at which the peak gain had been measured.

Conclusions

An experimental investigation of a gas dynamic laser has been made. During the course of the investigation both power and gain measurements have been made as a function of various parameters. As a result of the parameter study, a maximum gain of $1.0 \pm 0.04\%$ cm^{-1} and a maximum power of the order of 50 w at a flow rate of 0.7 mole/sec have been achieved. The magnitude of the maximum value of the experimental gain is in agreement with the results of independent theoretical calculations.

References

[1] Bosov, N. G. and Oraevski, A. N., "Attainment of Negative Temperatures by Heating and Cooling of a System," *Soviet Physics JETP*, Vol. 17, No. 5, Nov. 1963, pp. 1171–1172.

[2] Hurle, I. R. and Hertzberg, A., "Electronic Population Inversions by Fluid-Mechanical Techniques," *The Physics of Fluids*, Vol. 8, No. 9, Sept. 1965, pp. 1601–1607.

[3] Konyukhov, V. K. and Prokhorov, A. M., "Population Inversion in Adiabatic Expansion of a Gas Mixture," *JETP Letters*, Vol. 3, No. 1, Jan. 1966, pp. 286–288.

[4] Gerry, E. T., "Gas Dynamic CO_2 Lasers," American Physical Society Meeting Washington, D.C., April 1970.

[5] Konyukhov, V. K., Mastrosov, I. V., Prokhorov, A. M., Shulunov, D. T., and Shirokov, N. N., "Gas-dynamic CW Laser Using a Mixture of Carbon Dioxide, Nitrogen, and Water," *USSR Academy of Sciences, Zhurnal Eksperimental'noi i Theoreticheskoi Fiziki, Pis'ma u Redaktsiyu*, Vol. 12, Nov. 20, 1970, pp. 461–464.

[6] Lewis, J. W. L. and Lee, K. P., "Vibrational Relaxation in Carbon Dioxide/Water-Vapor Mixtures," *Journal of the Acoustical Society of America*, Vol. 38, July 1965, pp. 813–816.

[7] Shapiro, A. H., *The Dynamics and Thermodynamics of Compressible Fluid Flow*, Vol. II, Ronald Press, New York, 1954.

[8] Denes, L. J., "A Passively Stabilized CO Laser System," G130553-1, Dec. 1968, United Aircraft Corporation Research Labs., East Hartford, Conn.

[9] Rigrod, W. W., "Gain Saturation and Output Power of Optical Lasers," *Journal of Applied Physics*, Vol. 34, No. 9, Sept. 1963, pp. 2602–2609.

[10] Anderson, J. D., Jr., "Time-Dependent Analysis of Population Inversions in an Expanding Gas," *The Physics of Fluids*, Vol. 13, No. 8, Aug. 1970, pp. 1983–1989.

[11] Anderson, J. D., Jr., "A Time-Dependent Quasi-One-Dimensional Analysis of Population Inversions in an Expanding Gas," NOLTR 69-200, Dec. 1969. Naval Ordnance Lab., White Oak, Silver Spring, Md.

[12] Anderson, J. D., Jr., "Numerical Experiments Associated with Gas Dynamic Lasers," NOLTR 70-198, Sept. 1970, Naval Ordnance Lab., White Oak, Silver Spring, Md.

[13] Taylor, R. L. and Bitterman, S., "Survey of Vibrational Relaxation Data for Processes Important in the CO_2–N_2 Laser System," *Reviews of Modern Physics*, Vol. 41, No. 1, Jan. 1969, pp. 26–47.

[14] Sharma, R. D., "Vibrational Relaxation of CO_2 by H_2O," *Journal of Chemical Physics*, Vol. 54, No. 2, Jan. 1971, pp. 810–811.

[15] Patel, C. K. N., "Continuous-Wave Laser Action on Vibrational-Rotational Transitions of CO_2," *Physical Review*, Vol. 136, No. 5A, Nov. 30, 1964, pp. A1187–A1193.